The Cryosphere Open Access
Discussions

Dynamic ikaite production and dissolution in sea ice – control by temperature, salinity and pCO$_2$ conditions

S. Rysgaard[1,2,3,4], F. Wang[1,5], R. J. Galley[1], R. Grimm[6], M. Lemes[1],
N.-X. Geilfus[1], A. Chaulk[1], A. A. Hare[1], O. Crabeck[1], B. G. T. Else[1], K. Campbell[1],
T. Papakyriakou[1], L. L. Sørensen[4], J. Sievers[4,7], and D. Notz[6]

[1]Centre for Earth Observation Science, Department of Environment and Geography,
University of Manitoba, Winnipeg, MB R3T 2N2, Canada
[2]Department of Geological Sciences, University of Manitoba, Winnipeg, MB R3T 2N2, Canada
[3]Greenland Climate Research Centre, Greenland Institute of Natural Resources, 3900 Nuuk,
Greenland
[4]Arctic Research Centre, Aarhus University, 8000 Aarhus, Denmark
[5]Department of Chemistry, University of Manitoba, Winnipeg, MB R3T 2N2, Canada
[6]Max-Planck Institute for Meteorology, Hamburg, Germany
[7]Aarhus University, Department of Environmental Science, 4000 Roskilde, Denmark

Dynamic ikaite production and dissolution in sea ice

S. Rysgaard et al.

Title Page

Abstract	Introduction
Conclusions	References
Tables	Figures

|◄ ►|

◄ ►

Back Close

Full Screen / Esc

Printer-friendly Version

Interactive Discussion

Abstract

Ikaite is a hydrous calcium carbonate mineral ($CaCO_3 \cdot 6H_2O$). It is only found in a metastable state, and decomposes rapidly once removed from near-freezing water. Recently, ikaite crystals have been found in sea ice and it has been suggested that their precipitation may play an important role in air-sea CO_2 exchange in ice-covered seas. Little is known, however, of the spatial and temporal dynamics of ikaite in sea ice. Here we present evidence for highly dynamic ikaite precipitation and dissolution in sea ice grown at an out-door pool of the Sea-ice Environmental Research Facility (SERF). During the experiment, ikaite precipitated in sea ice with temperatures below −3 °C, creating three distinct zones of ikaite concentrations: (1) a mm to cm thin surface layer containing frost flowers and brine skim with bulk concentrations of $> 2000\,\mu mol\,kg^{-1}$, (2) an internal layer with concentrations of 200–$400\,\mu mol\,kg^{-1}$ and (3) a bottom layer with concentrations of $< 100\,\mu mol\,kg^{-1}$. Snowfall events caused the sea ice to warm, dissolving ikaite crystals under acidic conditions. Manual removal of the snow cover allowed the sea ice to cool and brine salinities to increase, resulting in rapid ikaite precipitation. The modeled (FREZCHEM) ikaite concentrations were in the same order of magnitude as observations and suggest that ikaite concentration in sea ice increase with decreasing temperatures. Thus, varying snow conditions may play a key role in ikaite precipitation and dissolution in sea ice. This will have implications for CO_2 exchange with the atmosphere and ocean.

1 Introduction

Throughout the last decade, sea-ice extent has decreased rapidly in the Arctic Ocean (e.g., Cavalieri and Parkinson, 2012). This Ocean represents an important sink for CO_2, with current estimates of net air-to-sea CO_2 fluxes at 66 to 199 $Tg\,C\,yr^{-1}$ (Bates and Mathis, 2009; Parmentier et al., 2013). To understand how the oceanic CO_2 sink will change with a reduced sea-ice cover, it is important to understand the driving factors

behind the air–sea exchange of CO_2. The precipitation of the metastable mineral ikaite ($CaCO_3 \cdot 6H_2O$) in polar sea ice may be critical in modifying the quantity of dissolved CO_2 in the surface ocean (pCO_2), with potentially important impacts on the global carbon cycle (Rysgaard et al., 2011).

5   Ikaite crystals have been reported in sea ice from both hemispheres (Dieckmann et al., 2008, 2010). However, the spatial and temporal dynamics of ikaite within sea ice is poorly known. Recent studies using microscopic imaging of sea ice thin sections to examine ikaite in situ have revealed ikaite crystals to concentrate in the interstices between the ice platelets in both granular and columnar sea ice (Rysgaard et al., 2013).

10 Their concentration appears to decrease from the ice surface towards the ice–water interface. Ikaite crystals are formed during winter conditions (Rysgaard et al., 2013; Geilfus et al., 2013a), but at present it is not known if they grow continuously during cold conditions or if they form and dissolve in response to variations in environmental conditions. Nonetheless, during summer it has been shown that dissolving ikaite

15 crystals from melting sea ice adds considerable amounts of total alkalinity (TA) to the surface waters thereby reducing surface water pCO_2 and increasing the potential for seawater uptake of CO_2 from the atmosphere (Rysgaard et al., 2012). Ikaite could have a major impact on air–sea CO_2 exchange rates if the crystals continually precipitate and dissolve in the winter. Thus, a better understanding of the dynamic ikaite

20 production and dissolution is needed.

Here, we present observations of ikaite conditions in newly formed sea ice, thin sea ice under different snow conditions, and in melting sea ice. In addition, we model ikaite concentrations using FREZCHEM (Marion, 2010) with seawater of varying initial compositions, and we discuss our findings in relation to CO_2 system dynamics in sea ice

25 covered seas.

2 Methods

2.1 Ice tank description, sampling and analysis

An experiment was performed at the Sea-ice Environmental Research Facility (SERF) at the University of Manitoba, Winnipeg, Canada, in an outdoor pool measuring 18.3 m by 9.1 m in surface area and 2.6 m in depth, with an approximate operating volume of 380 m^3. The pool was exposed to natural ambient temperatures, winds, and solar radiation, and contained artificial seawater (ASW) similar in chemical composition to natural average seawater reported by Millero (2006) (Table 1). Sea ice was grown in the pool from open water on 13 January (2013) and reached 20 cm in thickness on 26 January, after which the sea ice was melted by circulating heated ethylene glycol through a closed-loop hose fixed at the bottom of the pool.

Three events of snowfall occurred during the experiment. The first event occurred from 14–15 January, covering the sea ice surface with 1 cm of snow. The second event deposited 6–9 cm snow over the entire pool from 18–23 January. Then, on the morning of 23 January, the snow was manually cleared to investigate the insulating effect of snow on ice temperature and ikaite formation. This was followed by a final snowfall event, which began around noon on 24 January and deposited 8 cm of snow by 27 January, covering the entire pool until the end of the experiment on 30 January.

Ambient temperature (T) of seawater and bulk ice were recorded by automated type-T thermocouple arrays fixed into the outdoor pool, and 2 m air temperature and relative humidity were measured using a Vaisala HMP45C probe at a meteorological station located at the SERF site. Solar irradiance was continuously recorded by an Eppley Precision Spectral Pyranometer (range = 0.285–2.8 µm) mounted ∼ 10 m above the sea ice surface. In addition, estimated photosynthetically active radiation (PAR) values at the ice bottom was recorded with Alec mkv-L PAR sensors throughout the study and ranged from 0 to 892 µmol photons m^{-2} s^{-1}. Sea ice cores were extracted with a MARK II coring system (Kovacs Enterprises) and cut into 1 to 2 cm sections for bulk salinity analyses. Salinity (S) was determined from sample conductivity, T, and pres-

sure (P) as per Grasshoff et al. (1983). Ionic strength was calculated from the salinity ratio between the sample and standard seawater ($S = 35$, $I = 0.72\,\mathrm{mol\,kg^{-1}}$) assuming conservative behavior. Major ions (Na^+, Mg^{2+}, Ca^{2+}, K^+) were measured by inductively coupled plasma (ICP) optical emission spectroscopy (MCAL, University of Manitoba) and anions (Cl^-, SO_4^{2-}, Br^-) by ion chromatography (ALS Environmental, Winnipeg).

For analysis of ikaite, frost flowers (FF) and brine skim (BS) samples were collected with a pre-cleaned ceramic-bladed knife and transported cold in clean plastic bags to a cold laboratory ($-20\,^\circ$C) within 20 min. In addition, sea ice cores were extracted with a MARK II coring system and kept cold during the 20 min transport to a cold laboratory. Ice cores were collected from a bridge and it was not necessary to walk on the sea ice. Cores were collected from one end of the pool (half a meter away from the edge of the pool) and upwards during the campaign period. Cores were collected at least 20 cm away from previous cored sites. The bridge could be moved ensuring only undisturbed sea ice cores were collected. In the cold lab, sea ice cores were cut into 1–2 cm sections by a pre-cleaned stainless steel band saw. To document the abundance and concentrations of ikaite crystals in sea ice, 20–150 mg of sea ice were cut off using a ceramic-bladed knife at three random places within each sea ice section. An equal weight of BS was scraped from the ice surface layer of each core using a similar knife, and FF were carefully collected using two knives. The sea ice, BS and FF were weighed and placed onto a glass slide that rested on a chilled aluminum block with a 1 cm central viewing hole, then brought into a warm laboratory ($20\,^\circ$C). There they were inspected under a microscope (Leica DMiL LED equipped with a Leica DFC 295 camera and Leica Application Suite ver. 4.0.0. software) under 100–400 magnification as they were allowed to melt. A few seconds after the sea ice had melted the first image was taken. This image was used to document the amount and concentration of ikaite crystals (further details given below). After 2–5 min the second image was taken and compared with the first one (For further details, see Rysgaard et al., 2013). If crystals dissolved, they were assumed to be ikaite. Three photos, each covering 1.07 mm^2 of the counting area, were imaged in this fashion. The area of the melted sea ice sample

was determined after thawing to calculate the counted area to total area ratio. Ikaite crystals and other precipitates were observed to settle to the glass slide rapidly after ice crystal melt due to their high density. In total, three replicate sea ice sub-samples were processed from each sea ice section, resulting in 9 replicate images for each 1 to 2 cm vertical sea ice section, as well as for each FF and BS sample.

The abundance and concentration of crystals were calculated (only considering those that dissolves) from the images using the software ImageJ (1.45 s). Individual images were brightness, contrast and color adjusted prior to image analysis (see Rysgaard et al., 2013 for details) to convert to a binary image with crystals depicted as black on a white background. From this binary image, the area of ikaite crystals was calculated and converted to a volume using the relative dimensions of ikaite crystals (Rysgaard et al., 2012, see also Sect. 3). The mass and number of moles of ikaite crystals could then be determined from crystal density ($1.78\,\mathrm{g\,cm^{-3}}$), and molar weight ($208.18\,\mathrm{g\,mol^{-1}}$), which in turn permitted conversion to concentration (in $\mathrm{\mu mol\,kg^{-1}}$ melted sea ice) after carefully weighing the sample on a high-precision digital scale. Brine concentrations of ikaite were calculated from measured bulk ikaite concentrations divided by the brine volume. Brine volume was estimated from measurements of bulk salinity, temperature and density according to Cox and Weeks (1983).

Sea ice subsamples were also brought to an x-ray laboratory (Department of Geological Sciences at the University of Manitoba, Canada) within 20 min. There, 20–90 mg subsamples of sea ice were mounted onto a cold glass slide resting on a chilled aluminum block containing a 1 cm central viewing hole. Crystals were first examined with a polarized light microscope to assess their optical properties and then mounted for x-ray study using a stereo binocular microscope. Crystals were dragged across the cold glass slide using a metal probe and immersed into a drop of special purpose sampling oil that restricted sublimation. Each crystal was then scooped up with a low x-ray scattering micro-loop and instantly transferred to the nitrogen cold stream ($-10\,°\mathrm{C}$) on the x-ray diffraction instrument with a magnetic coupling goniometer head. The x-ray diffraction instrument consisted of a Bruker D8 three-circle diffractometer equipped with

Title Page

Abstract | Introduction

Conclusions | References

Tables | Figures

⏮ | ⏭

◀ | ▶

Back | Close

Full Screen / Esc

Printer-friendly Version

Interactive Discussion

a rotating anode generator (Mo K_α X-radiation), multi-layer optics, APEX-II CCD detector, and an Oxford 700 Series liquid-N Cryostream. The intensities of more than 100 reflections were harvested from six frame series (each spanning 15° in either ω or ϕ) collected to 60° 2θ using 0.6 s per 1° frame with a crystal-to-detector distance of 5 cm.

2.2 FREZCHEM modeling

Ikaite precipitation in sea ice was modeled by FREZCHEM (version 13.3), an equilibrium chemical thermodynamic model parameterized for concentrated solutions (up to 20 mol kg^{-1} (H$_2$O)) and sub-zero temperatures (down to −70 °C) (Marion and Kargel, 2008; Marion et al., 2010). The model uses the Pitzer approach to correct for activity coefficients of solutes in concentrated solutions. The FREZCHEM mineral database includes a variety of stable and metastable carbonate minerals of Ca (e.g., calcite, dolomite, aragonite, vaterite) (Marion, 2001). The solubility product of ikaite was based on the experimental data of Bischoff et al. (1993) extrapolated to low temperatures by Marion (2001). All other thermodynamic constants used were the default values provided by the model (Marion, 2001). The model inputs included the concentrations of all the major ions and the values of salinity and TA. Three types of seawater (Table 1) were considered: (1) SERF seawater ($S = 32.9$, TA = 2380 µmol kg^{-1}), (2) "standard seawater" ($S = 35$, TA = 2390 µmol kg^{-1}), (3) "seawater resembling bulk sea ice" ($S = 10$, TA = 800 µmol kg^{-1}, Rysgaard et al., 2009). Our calculation was done by following the seawater freezing from 0 to −16 °C at a step value of 0.5 °C. We assume that during the freezing process the system is always open to a constant pCO$_2$ = 390 µatm, and that solid phases precipitated at any given temperature are allowed to dissolve and re-precipitate as different solids when temperature changes ("equilibrium crystallization").

The FREZCHEM model simulates the formation of ice, along with other possible minerals, as seawater freezes in a system that is "closed" with respect to matter (e.g., no loss of salt to the underlying water column) except for gaseous components (in this case CO$_2$), which is allowed to transfer into or out of the system (Marion and Kargel, 2008). It considers both changes in concentrations due to brine volume changes,

and dependence of activity/thermodynamic constants on temperature. The modeling is based on the assumption that chemical species in the sea ice environment (ice, brine, and air) have reached thermodynamic equilibrium, and most of the thermodynamic constants used in the model were extrapolated to low temperatures rather than being determined experimentally. Nevertheless, the model has shown promising applications in exploring cold geochemical processes associated with seawater freezing (Marion et al., 1999, 2010) including the production of ikaite (Rysgaard et al., 2013).

3 Results

Figure 1 shows three examples of the crystals observed at SERF using the microscope imagery technique. Ikaite crystals become easily visible on the microscope in the laboratory when the sea ice melts. For example, the image shown in Fig. 1a consists of 159 crystals that were observed a few seconds after a 102 mg BS sample collected at 22 January 9 a.m. was melted. In this image, the crystal area covered 2.1 % of the counting area corresponding to an ikaite concentration of 4590 µmol kg^{-1}. Ikaite crystals at 2–3 cm depth (Fig. 1c) covered 0.4 % of the counting area corresponding to 950 µmol kg^{-1} and ikaite crystals at 9–10 cm depth (Fig. 1d) covered 0.05 % of the counting area corresponding to 90 µmol kg^{-1}. The crystals (a few µm to 100 µm in size) observed in the sea ice were highly transparent with a rhombic morphology and showed uniform extinction under cross-polarized light, suggesting that they were simple single crystals. All x-ray reflections fitted well to a monoclinic C-centered cell with $a\,(\text{Å}) = 8.816(14)$, $b\,(\text{Å}) = 8.317(9)$, $c\,(\text{Å}) = 11.042(2)$, $\beta\,(°) = 110.612(9)$, and $V\,(\text{Å}^3) = 757.8(3)$. From the general shape, optical properties and unit-cell determination, the crystals examined were confirmed to be ikaite (after Hesse and Küppers, 1983). Crystals shape varied (Fig. 1). To keep it as simple as possible we approximated ikaite volume as determined by its a, b, and c components above ($1 \times 1.06 \times 1.32$) assuming that crystals settled on the side with the largest area. The difference in estimation between a rectangular box and the unit cell from the x-ray analysis is less than 7 %.

Observations of atmospheric conditions, sea ice thickness, sea ice and water temperatures, salinity, and ikaite concentration are shown for the duration of the experiment in Fig. 2. Near the start of the experiment (13 January), air temperatures ranged from $-15\,°C$ to $-25\,°C$ (Fig. 2a), allowing rapid initial ice growth that reached a thickness of $\sim 5\,cm$ by the evening of 14 January (Fig. 2b). At that point the first ikaite crystals were observed in FF and BS (Fig. 2d), with concentrations in excess of $1000\,\mu mol\,kg^{-1}$ bulk ice (Fig. 2d). No ikaite crystals were observed in the ice column itself, which remained relatively warm (~ -2 to $-4\,°C$, Fig. 1b).

Initial sea ice growth in SERF occurred with ice attachment to the sides of the pool, resulting in the development of a hydrostatic pressure head that caused flooding of the sea ice surface between 15 and 18 January, and an increase in surface bulk ice salinity (Fig. 2c). Subsequently, cuts were made with a large saw around the perimeter of the pool to allow the ice to float, and a pressure release valve was installed to prevent further flooding. Over the same time period, a snow deposition event occurred, and ice temperatures in the top 5 centimeters oscillated between periods of relative warm ($\sim -3\,°C$) and cold ($\sim -7\,°C$, Fig. 1b). During a cold period on 14–15 January the first ikaite crystals in bulk ice were observed near the surface (Fig. 2d). A subsequent warming early on 16 January appeared to dissolve the crystals, which then reformed later in the day when ice temperatures dropped once again. Ikaite was also observed on the 18th near the bottom of the ice in a warmer, but more saline layer of the ice.

One m^2 of the surface was cleared from snow in the evening of 21 January to test how ikaite formation was affected. Ikaite was observed to form in high numbers on the surface ice in the morning of the 22 January. Thus, the surface of the entire sea ice was cleared of snow the morning of 23 January by shoveling. Air temperature during this time, and for the next two days, was cold at approximately $-22\,°C$ or lower. Shortly after the snow was removed, temperatures dropped significantly throughout the entire sea ice column, which had reached a thickness of over 20 cm at that time (Fig. 2b). Bulk salinities increased because of surface flooding and high ikaite concentrations were observed in FF, BS and the sea ice. Ikaite crystals in the ice were formed within several

Dynamic ikaite production and dissolution in sea ice

S. Rysgaard et al.

Title Page

Abstract | Introduction

Conclusions | References

Tables | Figures

◀ | ▶

◀ | ▶

Back | Close

Full Screen / Esc

Printer-friendly Version

Interactive Discussion

hours after snow clearing, indicating dynamic conditions of ikaite formation on short timescales. The highest FF and BS ikaite concentrations were recorded immediately prior to snow removal, in conjunction with a wet brine skim and snow mixture layer about 3 cm thick formed by the weight of the snow causing surface flooding, and very cold air temperatures in the nights of 20 and 21 January.

Shortly after the snow-clearing experiment, a third snowfall began at 12:00 h on the 24 January, covering the entire pool with 4–8 cm of dry snow by the 26 January. This resulted in an increase in sea ice temperature and reduced brine salinity. However, ikaite crystals concentrations remained high in the top 10 cm of the sea ice. After ice melt was initiated by turning on the heater on 26 January, sea ice temperatures rapidly increased and sea ice thickness rapidly decreased. This caused brine salinities to decrease and ikaite crystals in the sea ice to dissolve completely. The experiment was terminated on 30 January when sea ice had nearly disappeared.

4 Discussion

The ikaite concentrations in the present study are the highest reported from sea ice, with brine skim and frost flower concentrations of $> 2000\,\mu\text{mol}\,\text{kg}^{-1}$. These concentrations are several times higher than ikaite concentrations in FF and BS reported from Barrow, Alaska (max $25\,\mu\text{mol}\,\text{kg}^{-1}$, Geilfus et al., 2013a) but similar to FF and BS ikaite concentrations found in NE Greenland (500–$3000\,\mu\text{mol}\,\text{kg}^{-1}$, Barber et al., 2013). In this SERF study, frost flowers formed at air temperatures ranging from $-15\,°\text{C}$ to $-30\,°\text{C}$ and a relative humidity of 70–80 %. It is still not fully understood whether FF form due to deposition of atmospheric water vapour to the sea ice surface, or from sublimation of the warm ice surface into the atmospheric boundary layer, with recent research suggesting a dominating role of the latter (Style and Worster, 2009). In both cases, however, their fine structure provides a means of wicking surface brine toward the colder lower atmosphere (Roscoe et al., 2011). Evaporation to the atmosphere further concentrates the brines expelled to the ice surface and ikaite forms rapidly. Formation of

ikaite will result in CO_2 production according to the reaction:

$$Ca^{2+} + 2HCO_3^- + 5H_2O \leftrightarrow CaCO_3 \cdot 6H_2O + CO_2 \tag{R1}$$
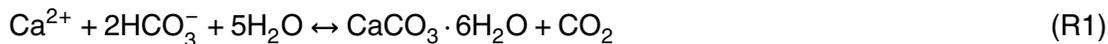
Most of this CO_2 formed on surface ice layers is likely released to the atmosphere, resulting in highly alkaline surface pH (Hare et al., 2013). Thus, our data add credibility to the suggestions by Rysgaard et al. (2011) and Geilfus et al. (2013a) that sea ice can act as a source of CO_2 to the atmosphere during cold conditions (and new ice formation). However, the ikaite being produced on the sea ice surface will, according to Eq. (1), take up an equal part of CO_2 when sea ice melts and mixes with ocean surface water and the ikaite crystals are dissolved. Hence, provided the ikaite dissolves in situ, the thin surface layer of sea ice should not have a net effect on the annual air–sea CO_2 flux, but instead represent a closed CO_2 loop where release and uptake are separated in time. If the sea ice surface is covered by snow shortly after frost flower formation, CO_2 may accumulate in the snow pack. Strong winds may then ventilate the snow pack and release this CO_2 to the atmosphere, which may explain some of the findings in the literature reporting high short-lived CO_2 fluxes during winter by eddy covariance (e.g., Papakyriakou and Miller, 2011; Miller et al., 2011; Else et al., 2011).

Even though ikaite concentrations in FF (note FF density is low, $0.02\,g\,cm^{-3}$; Domine et al., 2005) and the 1–2 mm thick BS are high, their importance to the total ikaite concentration in sea ice will decrease with increased sea ice thickness. They are also relatively short lived, occurring only over new and young sea ice under specific environmental conditions (e.g. Style and Worster, 2009). At maximum FF and BS concentrations (21–22 January), FF and BS would have accounted for 7–15 % of the total ikaite had they covered the entire SERF pond, whereas on 25 January they would have only accounted for 2–4 %. However, during the present experiment FF coverage was only 2 % making the relative contribution of FF to total ikaite concentration $\ll 1$ %. This is in general agreement with findings from field studies where FF and BS in newly formed (20 cm thick) sea ice fully covered by FF accounted for only 5 % of the total ikaite (Domine, 2005).

Title Page

Abstract | Introduction

Conclusions | References

Tables | Figures

|◀ | ▶|

◀ | ▶

Back | Close

Full Screen / Esc

Printer-friendly Version

Interactive Discussion

In order to assess if the observed relationship between sea ice temperature and ikaite concentrations measured in sea ice at SERF were chemically plausible, we employed the FREZCHEM model to calculate theoretical equilibrium ikaite concentrations as a function of different sea ice temperatures and seawater compositions (Fig. 3). Ikaite concentrations are reported as per mass of brine, since this should be the dominating control on ikaite abundance at a given temperature. The high FF and BS concentrations are not included in Fig. 3 because of their large density variations, which make comparisons by weight difficult. In the model run using SERF seawater (S = 32.9, TA = 2380 μmol kg^{-1}), ikaite starts to form at $-3\,°$C and increases to a concentration of $\sim 6000\,\mu$mol kg^{-1} brine at $-12\,°$C. The gray-shaded area in the plot shows the range of equilibrium ikaite concentrations modeled as seawater with different initial compositions freezes. This area is the expected range of equilibrium ikaite concentrations under two initial salinity and TA conditions: "standard seawater" ($S = 35$ and TA = 2390 μmol kg^{-1}; Millero, 2006) and "seawater resembling bulk sea ice" ($S = 10$, TA = 800 μmol kg^{-1}; as per Rysgaard et al., 2009). We choose these two compositions to bracket the expected ikaite concentration range, because the current version of FREZCHEM (13.3) treats the aqueous and solid phases as a closed system and cannot account for loss of salts to the underlying water during ice formation. The ikaite concentrations in SERF sea ice reported are in the same order of magnitude as the FREZCHEM model concentrations although the predictions are not impressive. Several sea ice layers were not observed to contain ikaite despite the fact that temperatures were below the model threshold of $-3\,°$C for the onset of ikaite formation and there seemed to be a delayed response for ikaite formation after snow clearance in the measurements compared to model simulations (we will discuss this further below).

The observed ikaite concentrations in the SERF sea ice (Fig. 2d), and the modeled concentrations from FREZCHEM (Fig. 3) suggest that ikaite concentration in the brine in general increase with decreasing temperatures. This is congruent with the understanding that cold sea ice temperatures cause reduced brine volume (e.g. Assur, 1960; Bennington, 1967; Lake and Lewis, 1970; Cox and Weeks, 1983; Perovich and

Gow, 1996; Cole and Shapiro, 1998; Eicken et al., 2000) and increased brine salinity, which in turn increases concentrations of Ca^{2+} and HCO_3^- sufficiently to allow for ikaite precipitation. The FREZCHEM model predicts that ikaite will not form until the temperature cools to a threshold of around -3 to $-5\,°C$. At that temperature or lower, the ion activity product (IAP) of $\{Ca^{2+}\}\{HCO_3^-\}^2\{H_2O\}^5/pCO_2$ in the brine equals to or exceeds the solubility product (K_{sp}) of ikaite due to freeze concentration, and thus ikaite starts to precipitate. A further decrease in temperature results in more ikaite being precipitated out from the brine, along with the precipitation of several other minerals such as mirabilite ($Na_2SO_4 \cdot 10H_2O$) and to a lesser extent gypsum ($CaSO_4 \cdot 2H_2O$) (Geilfus et al., 2013b). In the model, the production of ikaite plateaued around $-22\,°C$ after which the precipitation of hydrohalite ($NaCl \cdot 2H_2O$) significantly changed the brine chemistry with gypsum being the dominant calcium mineral.

An interesting observation here is that ikaite production after the snow clearing experiment (which lowered sea ice temperatures from -4 to $-14\,°C$) seemed to follow a similar slope as predicted by FREZCHEM at more moderate (-4 to $-7\,°C$) temperatures (Fig. 3). We interpret this as if the reaction rate can be slightly delayed relative to the rapid temperature change, causing ikaite precipitation to not instantaneously react to rapid temperature changes. Such delay is explicable through the possibly slightly delayed influence of temperature on brine volume, brine concentrations, and the availability of the reactants Ca^{2+} and HCO_3^-. Their response to any temperature change depends on an internal phase change, which requires the removal of latent heat. This, however, is a comparably slow process, which might explain the observed delay in the ikaite response. For slower temperature changes, however, temperature seems to be a rather direct control on ikaite concentration. A key implication of this dependence of ikaite concentration on temperature is that it is most likely not possible to quantify ikaite crystal concentrations accurately on sea ice cores that are kept frozen for later analysis at a temperature different from their in-situ temperature. Quantification of ikaite should hence be done rapid enough for the ice to retain its in situ temperature.

Although temperature (through its regulation of brine concentration) appears to control ikaite concentrations during the SERF experiment, there are several other processes that should be considered. Low ikaite concentrations were typically found in the lower middle part of the SERF sea ice where bulk salinities were lowest. These low ikaite concentrations were most likely due to inhibition of precipitation by low concentrations of Ca^{2+} and HCO_3^-, however another possibility is that crystals may have been lost to the underlying water column due to their relatively high density. This seems unlikely based on FREZCHEM modeling that predicts few crystals should form within these lower ice layers due to warmer temperatures. The low internal ikaite concentration could also be a result of ikaite dissolving due to slightly lower pH values caused by downward transport of pH equivalents originating from ikaite production in surface ice layers (see Hare et al., 2013 for further details on pH within sea ice). Biological impacts on ikaite crystal formation/dissolution are unlikely to have played a role in this experiment, as neither organic matter nor biota were purposely introduced into this experiments, and observed average levels of bulk ice microbial activity were very low $(1.12 \times 10^{-5}\,\mathrm{g\,C\,L^{-1}\,h^{-1}})$ and algal Chl a $(0.007\,\mathrm{\mu g\,L^{-1}})$ were very low.

The present study supports several key concepts described in a recent conceptual model on the processes driving air–sea gas exchange throughout the cycle of sea ice formation and decay (Rysgaard et al., 2011). First, the hypothesized release of CO_2 to the atmosphere during initial precipitation of ikaite in surface layers of the sea ice can be supported by our observations of high ikaite concentration in BS and FF. However, we do not observe a high CO_2 release to the air during this SERF experiment. Seems like most CO_2 goes down with the brine (Findings will be presented in a separate paper with gas fluxes and mass balance calculations from the entire pond). In SERF, ikaite formation seems to be high above the freeboard where temperatures are low and brine concentrations high. Secondly, the SERF experiment showed that ikaite crystals start to dissolve when temperatures start to rise and sea ice starts to melt. The quick dissolution of ikaite crystals in melting sea ice during this ice tank experiment supports

previous observations that sea ice melt water is severely CO_2 undersaturated relative to the atmosphere (Rysgaard et al., 2012; Else et al., 2013; Geilfus et al., 2012).

However, the SERF study also suggest that the process of ikaite precipitation and dissolution may occur multiple times between fall freeze-up and summer melt as a func-
tion of snow, temperature and pCO_2 conditions. Thus, dynamic conditions of ikaite crystals, CO_2 and pH are expected even during winter. This could have several implications for the exchange of carbonate species between sea ice and the underlying water. One possibility is that CO_2 released from ikaite precipitation in sea ice during cold periods is rejected to the underlying water. A new snowfall or a redistribution of
snow due to high winds to the same site may warm the sea ice cover locally. This will increase brine volumes, sea ice permeability, and the contact of the brine system with the underlying water, which depending on the pCO_2 conditions in the water column may dissolve ikaite. Dissolution of ikaite will increase TA and pH conditions in the near ice surface "melt-water". The overall outcome is that sea ice may be responsible for
low pCO_2 conditions in the ice-covered surface waters even in wintertime (e.g., Else et al., 2012). This mechanism of separating low pCO_2 surface waters from deeper high pCO_2 waters is supported by recent observations from a polynya site in NE Greenland where very low pCO_2 concentrations were observed near the sea ice–water interface (Rysgaard et al., 2013). Anther possibility is that ikaite form on the surface sea ice
layers via flooding and that CO_2 released from ikaite precipitation will be released to the atmosphere. Thus, melting of sea ice will not have a net effect on the CO_2 flux between air and seawater but rather take up the same amount of released CO_2 from the atmosphere. As a final remark, it should be mentioned that in any given sea ice area, several different sea ice stages of development (thicknesses) may be present at
one particular time as a result of broad scale sea ice dynamical processes. This means that the process of ikaite development can be at different stages in its evolution within a relatively small region.

Title Page

Abstract | Introduction

Conclusions | References

Tables | Figures

◄ | ►►

◄ | ►

Back | Close

Full Screen / Esc

Printer-friendly Version

Interactive Discussion

5 Conclusions

The ikaite concentrations in the present study are the highest reported from sea ice. Ikaite precipitated in sea ice with temperatures below $-3\,^{\circ}$C, creating three distinct zones of ikaite concentrations: (1) a mm to cm thin surface layer containing frost flowers and brine skim with bulk concentrations of $> 2000\,\mu mol\,kg^{-1}$, (2) an internal layer with localized concentrations of $200\text{--}400\,\mu mol\,kg^{-1}$ and (3) a bottom layer with concentrations of $< 100\,\mu mol\,kg^{-1}$. Snowfall events cause sea ice to warm leading to the dissolution of ikaite crystals under snow conditions. Removal of the snow cover allows the sea ice to cool and brine salinities to increase, resulting in rapid ikaite precipitation. Thus, varying snow conditions may play a key role in ikaite precipitation and dissolution at the surface of sea ice. This will have implications for CO_2 exchange with the atmosphere. The modeled ikaite concentrations from FREZCHEM are in the same order of magnitude as observations and suggest that ikaite concentration in sea ice may increase with decreasing temperatures. However, more developments on the FREZCHEM model are needed to accurately predict ikaite concentrations. Especially, it calls for the possible coupling of FREZCHEM to a model that can interactively simulate the loss of salts to the underlying water during ice formation.

References

Assur, A.: Composition of sea ice and its tensile strength, US Army Snow Ice and Permafrost Research Establishment, research report 44, Corps of Engineers, Wilmette, Illinois, 1960.

Title Page

Abstract | Introduction

Conclusions | References

Tables | Figures

|◄ | ►|

◄ | ►

Back | Close

Full Screen / Esc

Printer-friendly Version

Interactive Discussion

Barber, D. G., Ehn, J. K., Pucko, M., Deming, J., Rysgaard, S., Papakyriakou, T., Galley, R. J., and Søgaard, D.: Frost flowers on young sea ice: The climatic, chemical and microbial significance of an emerging ice type, in preparation, 2013.

Bates, N. R. and Mathis, J. T.: The Arctic Ocean marine carbon cycle: evaluation of air-sea CO_2 exchanges, ocean acidification impacts and potential feedbacks, Biogeosciences, 6, 2433–2459, doi:10.5194/bg-6-2433-2009, 2009.

Bennington, K. O.: Desalination features in natural sea ice, J. Glaciol., 6, 845–857, 1967.

Bischoff, J. L., Fitzpatrick, J. A., and Rosenbauer, R. J.: The solubility and stabilization of ikaite $(CaCO_3 \cdot 6H_2O)$ from 0° to 25°C: Environmental and paleoclimatic implications for thinolite tufa, J. Geol., 101, 21–33, 1993.

Cavalieri, D. J. and Parkinson, C. L.: Arctic sea ice variability and trends, 1979–2010, The Cryosphere, 6, 881–889, doi:10.5194/tc-6-881-2012, 2012.

Cole, D. M. and Shapiro, L. H.: Observations of brine drainage networks and microstructure of first-year sea ice, J. Geophys. Res., 103, 21739–21750, 1998.

Cox, G. F. N. and Weeks, W. F.: Equations for determining the gas and brine volumes in sea ice samples, J. Glaciol., 29, 306–316, 1983.

Dieckmann, G. S., Nehrke, G., Papadimitriou, S., Göttlicher, J., Steininger, R., Kennedy, H., Wolf-Gladrow, D., and Thomas, S. N.: Calcium carbonate as ikaite crystals in Antarctic sea ice, Geophys. Res. Lett., 35, L08501, doi:10.1029/2008GL033540, 2008.

Dieckmann, G. S., Nehrke, G., Uhlig, C., Göttlicher, J., Gerland, S., Granskog, M. A., and Thomas, D. N.: Brief Communication: Ikaite $(CaCO_3 \cdot 6 H_2O)$ discovered in Arctic sea ice, The Cryosphere, 4, 227–230, doi:10.5194/tc-4-227-2010, 2010.

Domine, F., Taillandier, A. S., Simpson, W. R., and Severin, K.: Specific surface area, density and microstructure of frost flowers, Geophys. Res. Lett., 32, L13502, doi:10.1029/2005GL023245, 2005.

Eicken, H., Bock, C., Wittig, R., Miller, H., and Poertner, H.-O.: Magnetic resonance imaging of sea-ice pore fluids: methods and thermal evolution of pore microstructure, Cold Reg. Sci. Technol., 31, 207–225, 2000.

Else, B. G. T., Papakyriakou, T. N., Galley, R. J., Drennan, W. M., Miller, L. A., and Thomas, H.: Wintertime CO_2 fluxes in an arctic polynya using eddy covariance: evidence for enhanced air–sea gas transfer during ice formation, J. Geophys. Res., 116, C00G03, doi:10.1029/2010JC006760, 2011.

Title Page

Abstract | Introduction

Conclusions | References

Tables | Figures

|◀ | ▶|

◀ | ▶

Back | Close

Full Screen / Esc

Printer-friendly Version

Interactive Discussion

Else, B. G. T., Papakyriakou, T. N., Galley, R. J., Mucci, A., Gosselin, M., Miller, L. A., Shadwick, E. H., and Thomas, H.: Annual cycles of $pCO_{2\,sw}$ in the southeastern Beaufort Sea: New understandings of air–sea CO_2 exchange in arctic polynya regions, J. Geophys. Res.-Oceans, 117, C00G13, doi:10.1029/2011JC007346, 2012.

Else, B. G. T., Galley, R. J., Lansard, B., Mucci, A., Papakyriakou, T. N., Brown, K., Tremblay, J.-É., Babb, D., Barber, D., Miller, L. A., and Rysgaard, S.: Further observations of a decreasing atmospheric CO_2 uptake capacity in the Canada Basin (Arctic Ocean) due to sea ice loss, Geophys. Res. Lett., 40, 1132–1137, doi:10.1002/grl.50268, 2013.

Geilfus, N.-X., Carnat, G., Papakyriakou, T., Tison, J.-L., Else, B., Thomas, H., Shadwick, E., and Delille, B.: Dynamics of pCO_2 and related air–ice CO_2 fluxes in the Arctic coastal zone (Amundsen Gulf, Beaufort Sea). J. Geophys. Res.-Oceans, 117, C00G10, doi:10.1029/2011JC007118, 2012.

Geilfus, N.-X., Carnat, G., Dieckmann, G. S., Halden, N., Nehrke, G., Papakyriakou, T., Tison, J.-L., and Delille, B.: First estimates of the contribution of $CaCO_3$ precipitation to the release of CO_2 to the atmosphere during young sea ice growth, J. Geophys. Res.-Oceans, 118, 1–12, doi:10.1029/2012JC007980, 2013a.

Geilfus, N.-X., Galley, R. J., Hare, A., Wang, F., Søgaard, D., and Rysgaard, S.: Ikaite and gypsum crystals observed in experimental and natural sea ice, J. Glaciol., accepted, 2013b.

Grasshoff, K., Erhardt, M., and Krembling, K.: Methods of Seawater Analysis, 2nd revised and extended version, Weinheim, Nürnberg, Germany, 1983.

Hare, A., Wang, F., Barber, D., Geilfus, N.-X., Galley, R. J., and Rysgaard, S.: pH evolution in sea ice grown at an outdoor experimental facility, Mar. Chem., 154, 46–54, doi:10.1016/j.marchem.2013.04.007, 2013.

Hesse, K. F. and Küppers, H.: Refinement of the structure of Ikaite, $CaCO_3 \cdot 6\,H_2O$, Z. Kristallogr., 163, 227–231, 1983.

Lake, R. A. and Lewis, E. L.: Salt rejection by sea ice during growth, J. Geophys. Res., 75, 583–597, 1970.

Marion, G. M.: Carbonate mineral solubility at low temperatures in the Na–K–Mg–Ca–H–Cl–SO_4–OH–HCO_3–CO_3–CO_2–H_2O system, Geochim. Cosmochim. Ac., 65, 1883–1896, 2001.

Marion, G. M. and Kargel, J. S.: Cold Aqueous Planetary Geochemistry with FREZCHEM: from Modeling to the Search for Life at the Limits, Springer, Heideberg, 251 pp., 2008.

Marion, G. M., Farren, R. E., and Komrowski, A. J.: Alternative pathways for seawater freezing, Cold Reg. Sci. Technol., 29, 259–266, 1999.

Marion, G. M., Mironenko, M. V., and Roberts, M. W.,: FREZCHEM: a geochemical model for cold aqueous solutions, Comput. Geosci., 36, 10–15, 2010.

Miller, L., Papakyriakou, T., Collins, R. E., Deming, J., Ehn, J., Macdonald, R. W., Mucci, A., Owens, O., Raudsepp, M., and Sutherland, N.: Carbon dynamics in sea ice: a winter flux time series, J. Geophys. Res.-Oceans, 116, C02028, doi:10.1029/2009JC006058, 2011.

Millero, F. J.: Chemical Oceanography, CRC press, 30, 2006.

Papakyriakou, T. and Miller, L.: Springtime CO_2 exchange over seasonal sea ice in the Canadian Arctic Archipelago, Ann. Glaciol., 52, 215–224, 2011.

Parmentier, F. J. W., Christensen, T. R., Sørensen, L. L., Rysgaard, S., McGuire, A. D., Miller, P. A., and Walker, D. A.: The impact of a lower sea-ice extent on Arctic greenhouse-gas exchange, Nature Clim. Change, 3, 195–202, doi:10.1038/nclimate1784, 2013.

Perovich, D. K. and Gow, A. J.: A quantitative description of sea ice inclusions, J. Geophys. Res., 101, 18327–18343, 1996.

Roscoe, H. K., Brooks, B., Jackson, A. V., Smith, M. H., Walker, S. J., Obbard, R. W., and Wolff, E. W.: Frost flowers in the laboratory: growth, characteristics, aerosol and the underlying sea ice, J. Geophys. Res., 116, D12301, doi:10.1029/2010JD015144, 2011.

Rysgaard, S., Bendtsen, J., Delille, B., Dieckmann, G., Glud, R. N., Kennedy, H., Mortensen, J., Papadimitriou, S., Thomas, D., and Tison, J.-L.: Sea ice contribution to air–sea CO_2 exchange in the Arctic and Southern Oceans, Tellus B, 63, 823–830, doi:10.1111/j.1600-0889.2011.00571.x, 2011.

Rysgaard, S., Bendtsen, J. B., Pedersen, L. T., Ramløv, H., and Glud, R. N.: Increased CO_2 uptake due to sea-ice growth and decay in the Nordic Seas, J. Geophys. Res., 114, C09011, doi:10.1029/2008JC005088, 2009.

Rysgaard, S., Glud, R. N., Lennert, K., Cooper, M., Halden, N., Leakey, R. J. G., Hawthorne, F. C., and Barber, D.: Ikaite crystals in melting sea ice – implications for pCO_2 and pH levels in Arctic surface waters, The Cryosphere, 6, 901–908, doi:10.5194/tc-6-901-2012, 2012.

Rysgaard, S., Søgaard, D. H., Cooper, M., Pućko, M., Lennert, K., Papakyriakou, T. N., Wang, F., Geilfus, N. X., Glud, R. N., Ehn, J., McGinnis, D. F., Attard, K., Sievers, J., Deming, J. W., and Barber, D.: Ikaite crystal distribution in winter sea ice and implications for CO_2 system dynamics, The Cryosphere, 7, 707–718, doi:10.5194/tc-7-707-2013, 2013.

Title Page

Abstract | Introduction

Conclusions | References

Tables | Figures

◄◄ | ►►

◄ | ►

Back | Close

Full Screen / Esc

Printer-friendly Version

Interactive Discussion

Style, R. W. and Worster, M. G.: Frost flower formation on sea ice and lake ice, Geophys. Res. Lett., 36, L11501, doi:10.1029/2009GL037304, 2009.

Title Page

Abstract | Introduction

Conclusions | References

Tables | Figures

|◀ | ▶|

◀ | ▶

Back | Close

Full Screen / Esc

Printer-friendly Version

Interactive Discussion

Table 1. Seawater composition used in the FREZCHEM modeling.

Composition	SERF seawater (Ex 2.2)	Standard seawater[a]	Seawater resembling bulk sea ice[b]
Na^+ (mol kg^{-1})	0.4719	0.48606	0.1392
K^+ (mol kg^{-1})	0.009796	0.01058	0.0032
Ca^{2+} (mol kg^{-1})	0.011478	0.01066	0.0030457
Mg^{2+} (mol kg^{-1})	0.026167	0.05474	0.01564
Cl^- (mol kg^{-1})	0.5134	0.56577	0.16165
Br^- (mol kg^{-1})	0.0009236	0.00087	0.00024858
SO_4^{2-} (mol kg^{-1})	0.02021	0.02926	0.00836
TA (µmol kg^{-1})	2380	2390	800
S	32.9	35	10

[a] Based on Millero (2006).
[b] Extrapolated from the $S = 35$ standard seawater to $S = 10$.
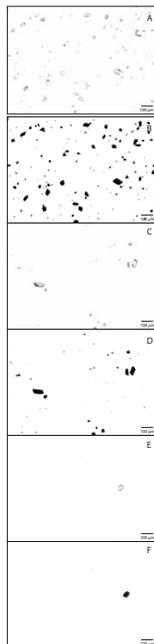
Fig. 1. Microscopic images of ikaite crystals **(A)** a few seconds after melting 102 mg sea ice (brine skim sample) from 22 January. Image represents a very small fraction (3 µg) of the sample. **(B)** Software (ImageJ 1.45 s) processing of image **(A)** to find the number (159) and area (2.1 % of counting area) of the crystals. Microscopic images of ikaite crystals **(C)** a few seconds after melting 86 mg sea ice (from 2 cm depth) from 22 January. Image represents a very small fraction (3 µg) of the sample. **(D)** Software processing of image **(C)** to find the number (31) and area (0.4 % of counting area) of the crystals. Microscopic images of ikaite crystals **(E)** a few seconds after melting 42 mg sea ice (from 10 cm depth) from 22 January. Image represents a very small fraction (3 µg) of the sample. **(F)** Software processing of image **(E)** to find the number (1) and area (0.05 % of counting area) of the crystals.
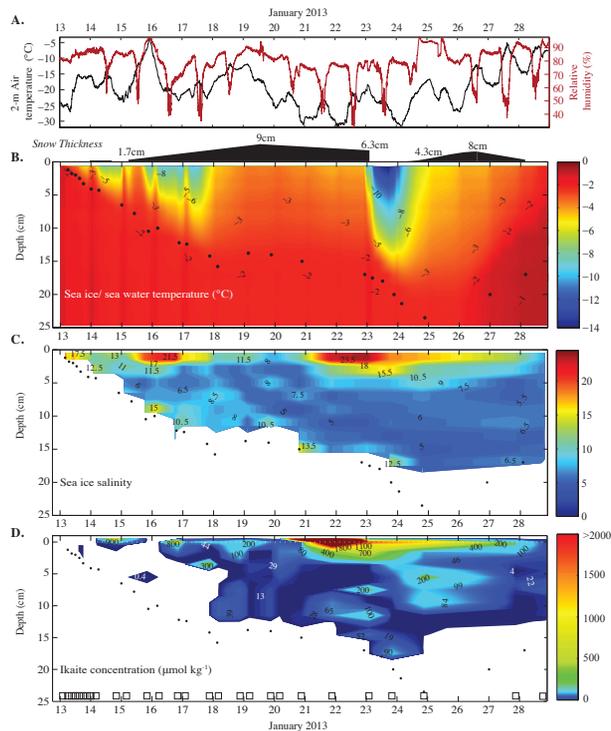
Fig. 2. (A) Air temperature (black lines), relative humidity (red lines), **(B)** snow cover (black horizontal bars), and sea ice/water temperature (°C), **(C)** bulk ice salinity (psu) and **(D)** bulk ikaite concentration (µmol kg^{-1} sea ice) in experimental sea ice grown at the Sea-ice Environmental Research Facility (SERF) during 13–30 January 2013. In **(D)**, the horizontal dotted line in upper sea ice layers (above 0) represents the BS and FF layer. In panels **(B)** to **(D)**, sea ice thickness is illustrated by black dots. Open squares in the lower part of **(D)** mark the sampling times of ikaite.

Title Page

Abstract | Introduction

Conclusions | References

Tables | Figures

|◄ | ►|

◄ | ►

Back | Close

Full Screen / Esc

Printer-friendly Version

Interactive Discussion
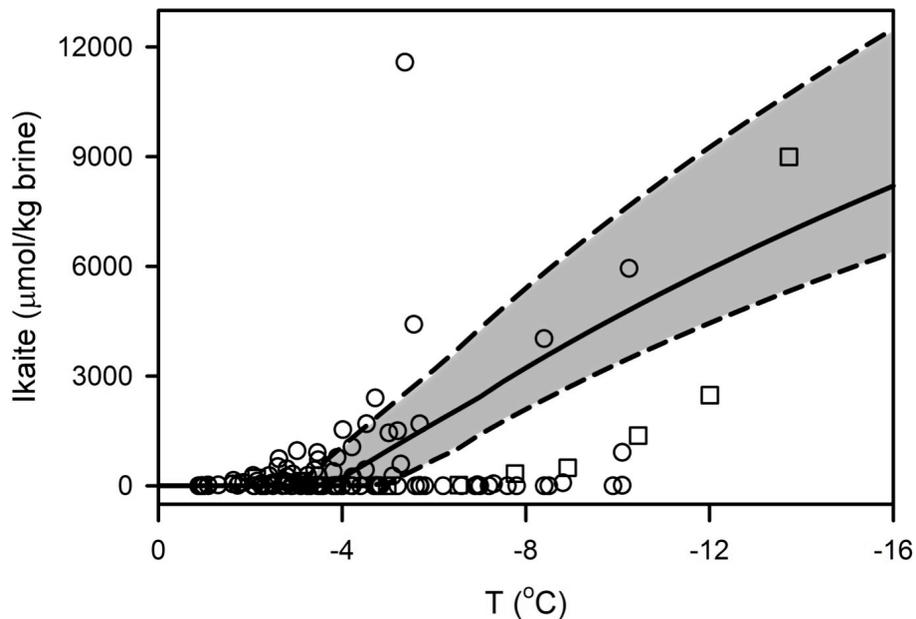
Fig. 3. Abundance of ikaite in sea ice, expressed as mass of ikaite per mass of brine, as a function of temperature. Symbols are observed ikaite concentrations at SERF (circles: measurement within 30 min of sample collection; squares: samples taken on 24 January after the manual snow clearance). The grey-shaded area shows the range of equilibrium ikaite concentrations modeled by FREZCHEM, as seawater with different initial compositions (lower dashed line: "standard seawater" with $S = 35$, TA = 2390 µmol kg^{-1}; upper dashed line: seawater resembling bulk sea ice with $S = 10$, TA = 800 µmol kg^{-1}) freezes from 0 to -16 °C while open to the atmospheric $p\text{CO}_2 = 390$ µatm. The solid line is equilibrium ikaite concentration modeled by FREZCHEM based on SERF seawater composition ($S = 32.9$, TA = 3280 µmol kg^{-1}) at $p\text{CO}_2 = 390$ µatm.